Double parton distributions in colour space.

Perturbative splitting and positivity bounds.

[arXiv:2105.08425, arXiv:2109.14304]

November 15, 2021

M. Diehl [1]   J. R. Gaunt [2]   P. Plößl [1]

[1]Deutsches Elektronen-Synchrotron DESY
[2]Department of Physics and Astronomy, University of Manchester

Colour structure of DPDs.

[arXiv:2105.08425]

[arXiv:2109.14304]

Coupling of colour indices for DPDs.

In contrast to PDFs DPDs exhibit a rich colour structure:

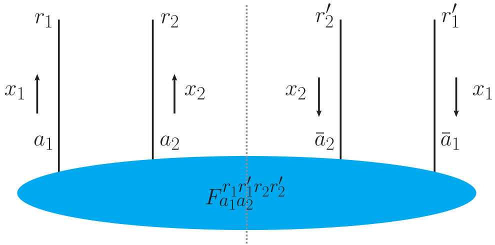

$\longrightarrow$ decompose DPDs in terms of distributions projected onto definite colour representations!

Coupling of colour indices for DPDs.

In contrast to PDFs DPDs exhibit a rich colour structure:

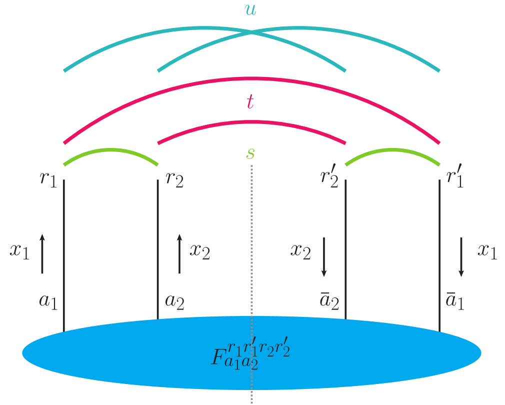

$\longrightarrow$ decompose DPDs in terms of distributions projected onto definite colour representations!

Coupling of colour indices for DPDs.

In contrast to PDFs DPDs exhibit a rich colour structure:

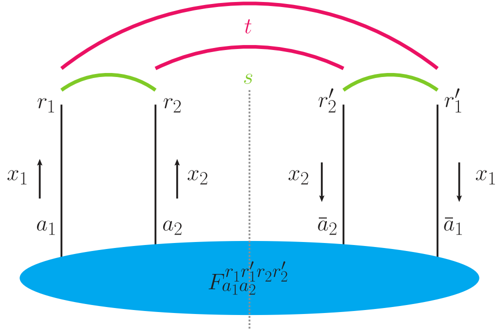

$\longrightarrow$ decompose DPDs in terms of distributions projected onto definite colour representations!

t- and s-channel DPDs.

In the t-channel the colour indices r_i and r_i' are coupled to an irreducible representation R_i of $SU(N)$ such that R_1R_2 is a singlet:

$$^{R_1R_2}F_{a_1a_2} \sim P^{r_1r_1'\,r_2r_2'}_{\overline{R}_1\overline{R}_2} F^{r_1r_1'r_2r_2'}_{a_1a_2} \qquad \text{such that} \qquad F^{r_1r_1'r_2r_2'}_{a_1a_2} \sim \sum_{R_1,R_2} P^{r_1r_1'\,r_2r_2'}_{R_1R_2}\; {}^{R_1R_2}F_{a_1a_2}$$

In the s-channel the colour indices r_1 and r_2 are coupled to an irreducible representation R and r_1' while r_2' are coupled to R' such that RR' is again a singlet:

$$F^{RR'}_{a_1a_2} \sim P^{r_1r_2\,r_1'r_2'}_{\overline{R}\overline{R}'} F^{r_1r_1'r_2r_2'}_{a_1a_2} \qquad \text{such that} \qquad F^{r_1r_1'r_2r_2'}_{a_1a_2} \sim \sum_{R,R'} P^{r_1r_2\,r_1'r_2'}_{RR'}\; F^{RR'}_{a_1a_2}$$

Note that the exact form of $F^{RR'}_{a_1a_2}$ and $^{R_1R_2}F_{a_1a_2}$ depends on the choice of normalisation.

Colour non-singlet splitting DPDs at NLO.

[arXiv:2105.08425]

Perturbative splitting in DPDs.

In the limit of small distance $\boldsymbol{y}$ the leading contribution to a DPD is due to the perturbative splitting of one parton into two and can be calculated in perturbation theory:

$$ {}^{R_1R_2}F_{a_1a_2}(x_i, y, \zeta_p, \mu) \overset{y\to 0}{=} \frac{1}{\pi y^2} \left[{}^{R_1R_2}V_{a_1a_2,a_0}(y, \zeta_p, \mu) \underset{12}{\otimes} f_{a_0}(\mu) \right](x_i)\,, $$

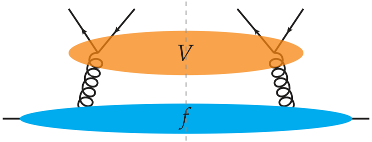

where

$$ \left[V \underset{12}{\otimes} f\right](x_i) = \int_x^1 \frac{dz}{z^2}\, V\!\left(\frac{x_1}{z}, \frac{x_2}{z}\right) f(z) $$

LO kernels for all R_1R_2 can be found in [Diehl, Ostermeier, and Schäfer, 2012].

NLO kernels for $R_1R_2 = 11$ have been calculated in [Diehl, Gaunt, Plößl, and Schäfer, 2019].

Colour non-singlet splitting DPDs at NLO.

Many ingredients from the calculation of the colour singlet splitting in [Diehl, Gaunt, Plößl, and Schäfer, 2019] can be reused for the colour non-singlet case: diagrams, master integrals, Dirac algebra.

In the colour non-singlet case rapidity divergences no longer cancel after a sum over graphs and have to be treated with utmost care. For this we use two regulators:

- Collins regulator using space-like Wilson lines. [Collins, 2011]
- δ regulator. [Echevarria, Scimemi and Vladimirov, 2016]

After combining the splitting DPDs calculated with these regulators with the DPS soft factor we find matching results in both schemes!

$\longrightarrow$ First application (to our knowledge) of the Collins regulator to a two loop calculation!

Small-y limit of DPDs.

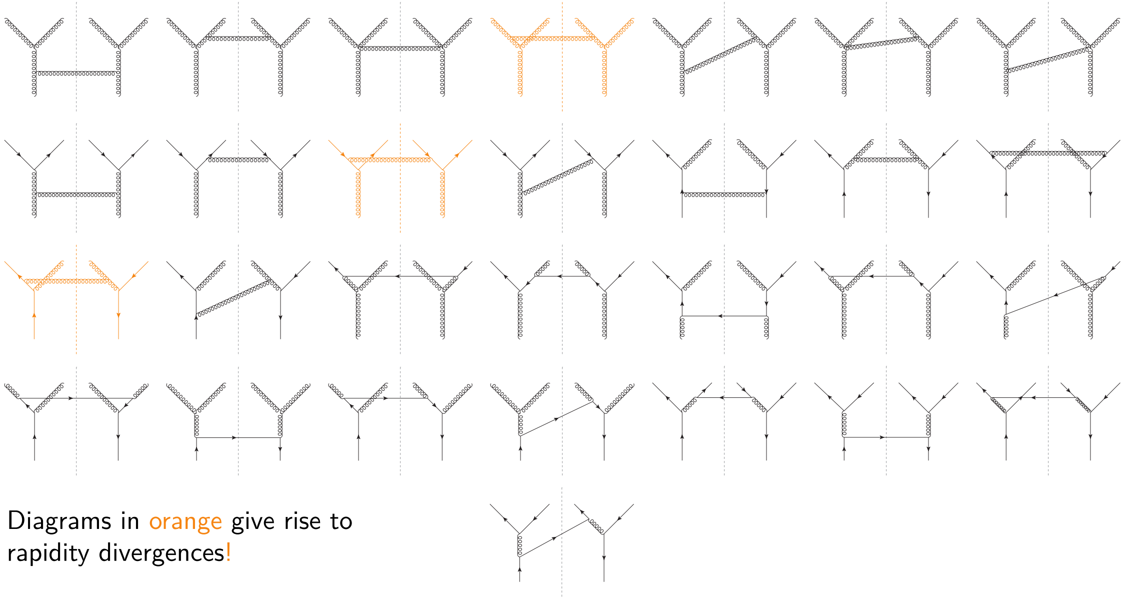

Diagrams in orange give rise to rapidity divergences!

Small-y limit of DPDs.

Diagrams in orange give rise to rapidity divergences!

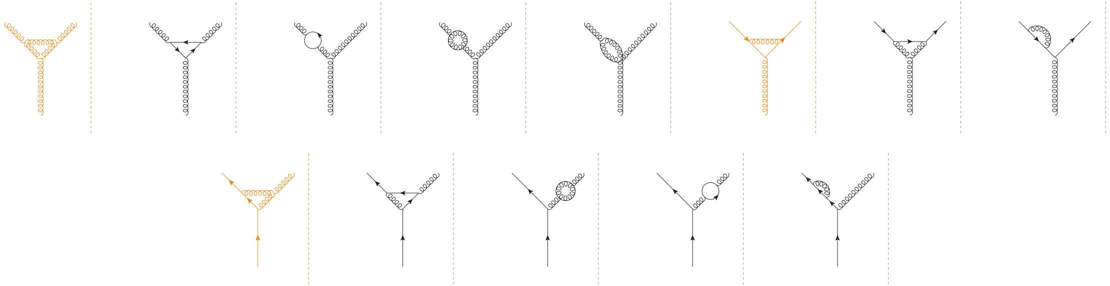

General structure of NLO colour non-singlet kernels.

Colour non-singlet kernels:

$$
\begin{aligned}
{}^{R_1R_2}V^{(2)}_{a_1a_2,a_0}(z,u,y,\mu,\zeta) &= {}^{R_1R_2}V^{[2,0]}_{a_1a_2,a_0}(z,u) + L\ {}^{R_1R_2}V^{[2,1]}_{a_1a_2,a_0}(z,u) \\
&\quad + \left(L \log\frac{\mu^2}{\zeta} - \frac{L^2}{2} + c_{\overline{\text{MS}}}\right) \frac{{}^{R_1}\gamma_J^{(0)}}{2}\ {}^{R_1R_2}V^{(1)}_{a_1a_2,a_0}(z,u)
\end{aligned}
$$

where $L = \log\frac{y^2\mu^2}{b_0^2}$ and $b_0 = 2e^{-\gamma}$ and

$$
{}^{R_1R_2}V^{[2,0]}(z,u) = {}^{R_1R_2}V^{[2,0]}_{\text{regular}}(z,u) + \delta(1-z)\,{}^{R_1R_2}V^{[2,0]}_{\delta}(u)\,,
$$

$$
{}^{R_1R_2}V^{[2,1]}(z,u) = {}^{R_1R_2}V^{[2,1]}_{\text{regular}}(z,u) + \frac{1}{[1-z]_+}\,{}^{R_1R_2}V^{[2,1]}_{+}(u) + \delta(1-z)\,{}^{R_1R_2}V^{[2,1]}_{\delta}(u)
$$

In contrast to the LO case there are – with few exceptions – no simple scaling relations between different colour channels!

Impact of NLO corrections on small y DPDs.

We study how including the NLO corrections effects the small y gg DPD for the following set of parameters:

- $y = 0.022\,\mathrm{fm}$
- $\mu = \frac{b_0}{y} = 10\,\mathrm{GeV}$
- $x_1 x_2 \zeta_p = \mu^2 = 100\,\mathrm{GeV}^2$

For this choice of parameters only the $V^{[2,0]}$ part of the kernels contributes to the final DPD.

In order to get a feeling for the relative importance of the logarithmic $V^{[2,1]}$ and double logarithmic $V^{(1)}$ parts we vary μ and $\sqrt{x_1 x_2 \zeta_p}$ by a factor of two around their central values.

Small-y limit of DPDs.

$|x_1 x_2\, {}^{RR}F_{gg}|$.

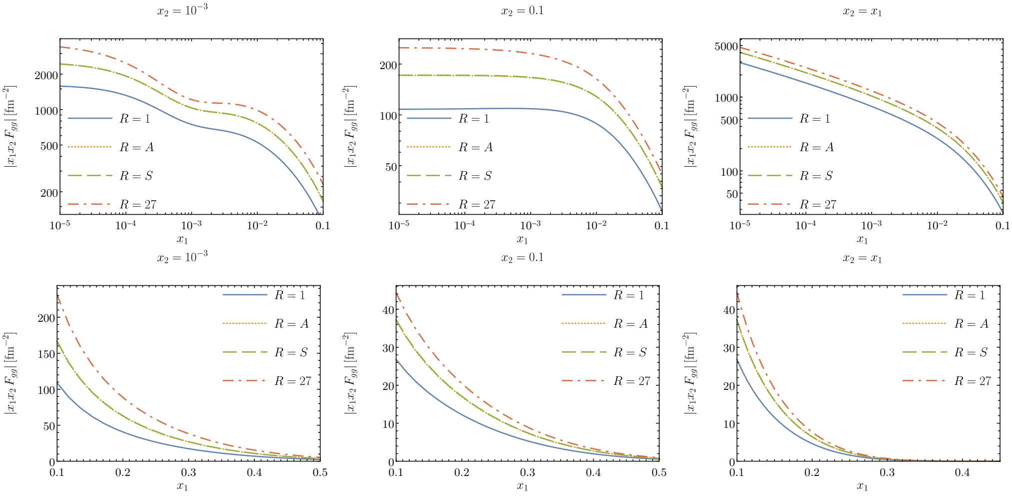

${}^{RR}F_{gg}^{(2)} \,/\, {}^{RR}F_{gg}^{(1)}$.

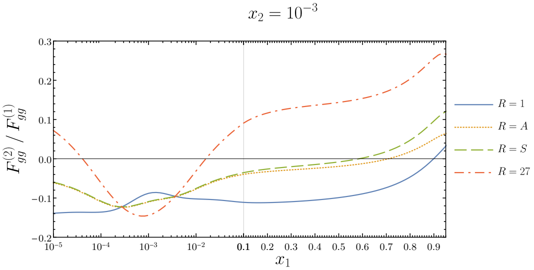

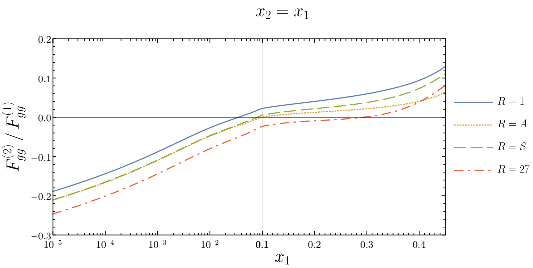

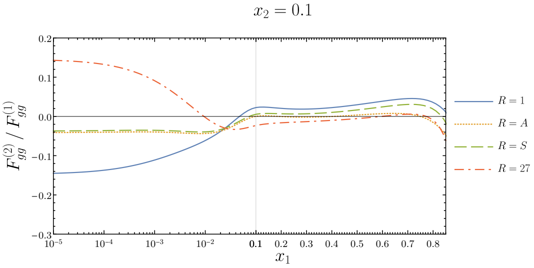

- moderate ($\mathcal{O}(10\%)$) NLO corrections.
- varied structure as a function of x_1 and x_2.
- results rather independent of PDF sets used.

Small-y limit of DPDs.

${}^{RR}F_{gg}^{(2)} \, / \, {}^{RR}F_{gg}^{(1)}$.

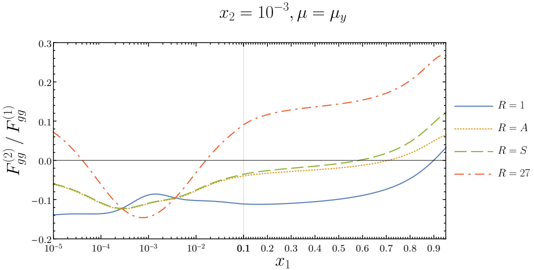

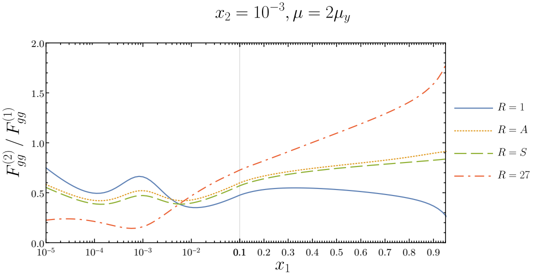

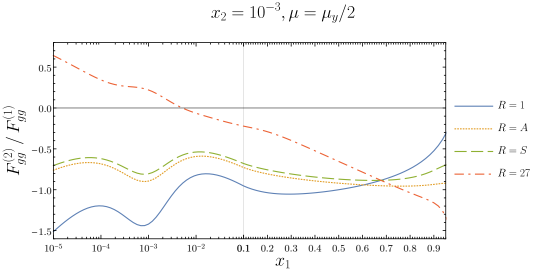

- large ($\mathcal{O}(100\%)$) NLO corrections for $\mu \neq \mu_y$.
- splitting form should be evaluated at $\mu \sim \mu_y$ to avoid large higher order corrections.

Violation of positivity bounds for s-channel DPDs.

[arXiv:2109.14304]

Introduction.

s-channel DPDs $F^{R\overline{R}}_{a_1 a_2}$ allow a density interpretation as the probability to find the parton pair $a_1 a_2$ in any of the $m(R)$ states of representation R. [Kasements and Mulders, 2014]

This interpretation results in the following positivity bound for s-channel DPDs:

$$F^{R\overline{R}}_{a_1 a_2} \geq 0$$

for all representations R and parton combinations $a_1 a_2$.

Check if these bounds are violated:

- Consider the small-y regime where DPDs are known from perturbation theory.
- Restrict discussion to quark-quark and quark-antiquark distributions (comparatively simple colour structure).
- Consider s-channel DPDs that vanish at LO: $F^{\overline{3}3}_{qq}$, $F^{6\overline{6}}_{qq}$, $F^{\overline{3}3}_{qq'}$, $F^{6\overline{6}}_{qq'}$, $F^{11}_{q\bar{q}}$, $F^{11}_{q\bar{q}'}$, $F^{88}_{q\bar{q}'}$.

NLO s-channel splitting DPDs.

Using the same numerical setup as for the study of the t-channel NLO splitting contributions one can explicitly check whether the s-channel NLO splitting DPDs can violate positivity.

Consider to this end distributions with vanishing LO contributions:

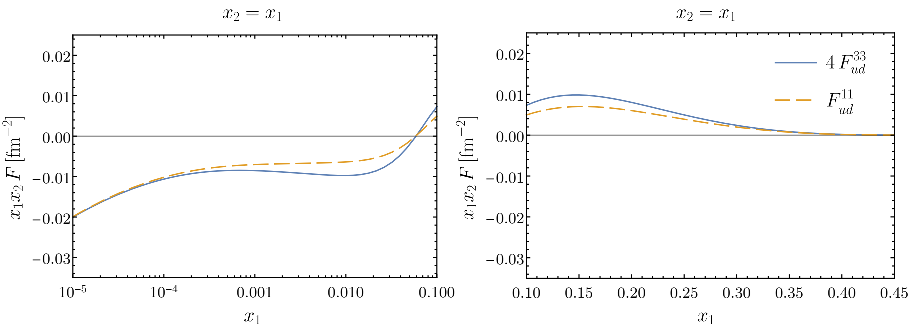

$$\mu = \mu_y/1.2$$

NLO s-channel splitting DPDs.

Using the same numerical setup as for the study of the t-channel NLO splitting contributions one can explicitly check whether the s-channel NLO splitting DPDs can violate positivity.

Consider to this end distributions with vanishing LO contributions:

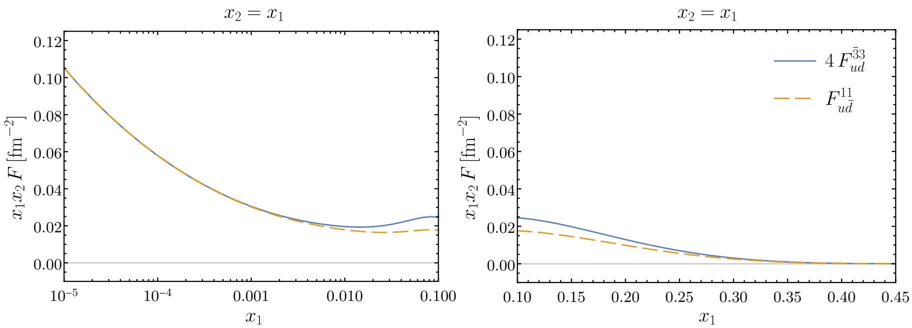

$$\mu = \mu_y$$

NLO s-channel splitting DPDs.

Using the same numerical setup as for the study of the t-channel NLO splitting contributions one can explicitly check whether the s-channel NLO splitting DPDs can violate positivity.

Consider to this end distributions with vanishing LO contributions:

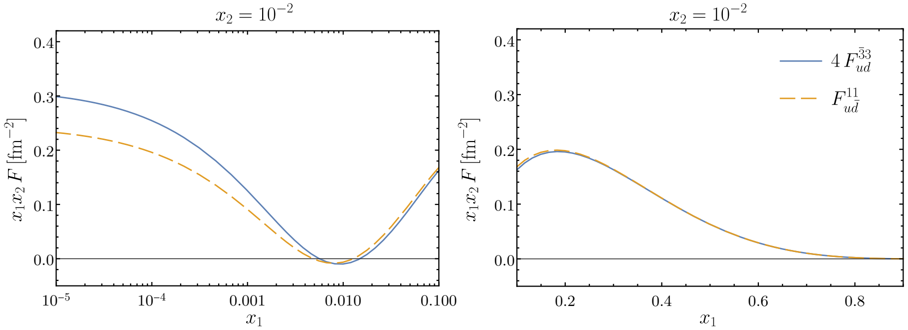

$$\mu = \mu_y/1.2$$

NLO s-channel splitting DPDs.

Using the same numerical setup as for the study of the t-channel NLO splitting contributions one can explicitly check whether the s-channel NLO splitting DPDs can violate positivity.

Consider to this end distributions with vanishing LO contributions:

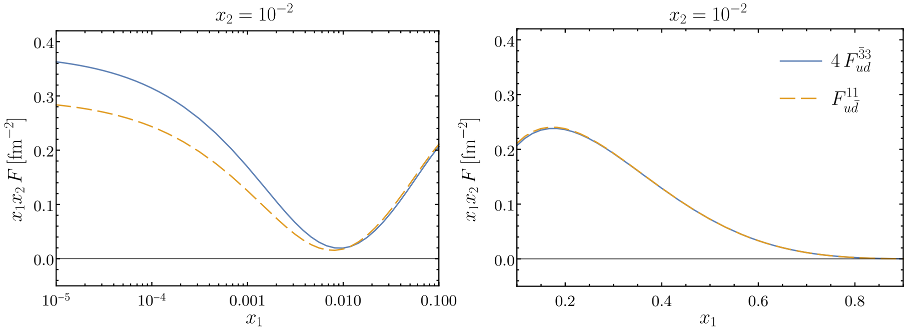

$$\mu = \mu_y$$

NLO s-channel splitting DPDs.

Using the same numerical setup as for the study of the t-channel NLO splitting contributions one can explicitly check whether the s-channel NLO splitting DPDs can violate positivity.

Consider to this end distributions with vanishing LO contributions:

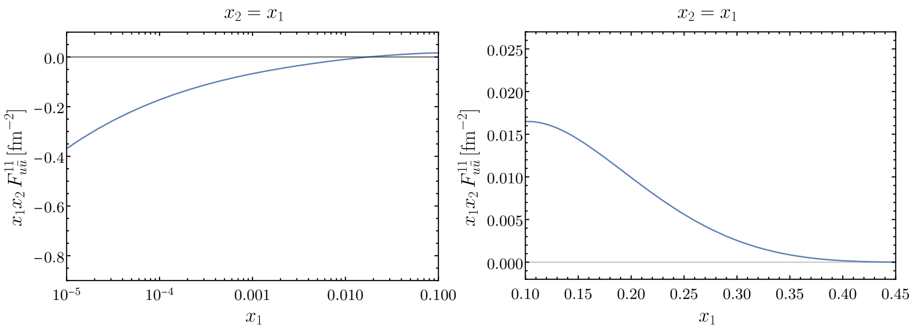

$$\mu = \mu_y$$

NLO s-channel splitting DPDs.

Using the same numerical setup as for the study of the t-channel NLO splitting contributions one can explicitly check whether the s-channel NLO splitting DPDs can violate positivity.

Consider to this end distributions with vanishing LO contributions:

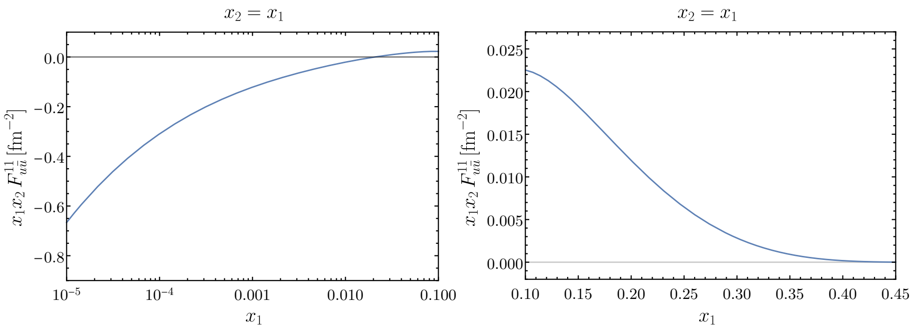

$$\mu = 1.2\mu_y$$

NLO s-channel splitting DPDs.

Using the same numerical setup as for the study of the t-channel NLO splitting contributions one can explicitly check whether the s-channel NLO splitting DPDs can violate positivity.

Consider to this end distributions with vanishing LO contributions:

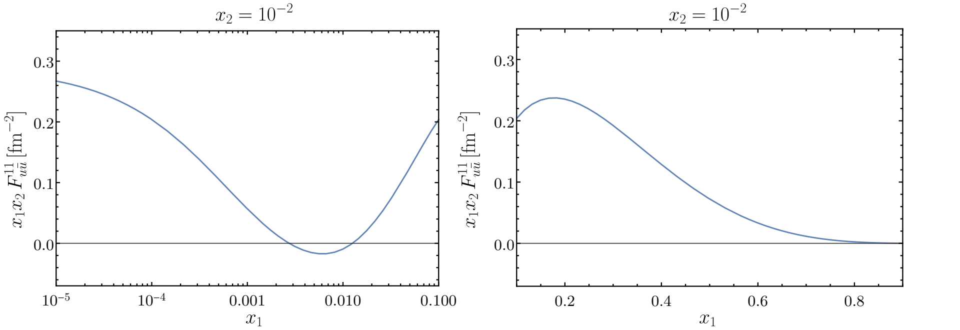

$$\mu = \mu_y$$

NLO s-channel splitting DPDs.

Using the same numerical setup as for the study of the t-channel NLO splitting contributions one can explicitly check whether the s-channel NLO splitting DPDs can violate positivity.

Consider to this end distributions with vanishing LO contributions:

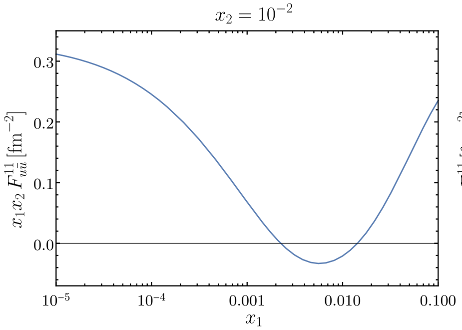

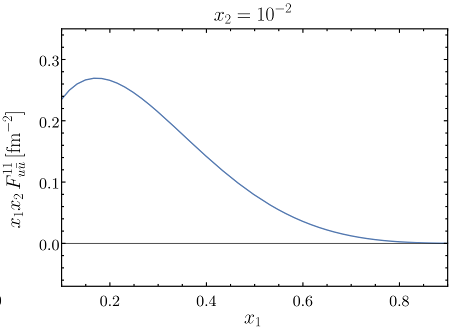

$$\mu = 1.2\mu_y$$

Violation of positivity from DGLAP evolution.

Evolution of s-channel DPDs.

One can show that positivity is not necessarily conserved under LO DGLAP evolution.

Consider to this end one of the small-y s-channel distributions which are zero at LO: $F^{11}_{q\bar{q}}$.

The double DGLAP equation is most naturally formulated in the t-channel, where it reads:

$$\frac{\partial}{\partial \log \mu_1^2} {}^{R_1 R_2}F_{q\bar{q}}(x_i, \boldsymbol{y}, \zeta_p, \mu_i) = \left[{}^{R_1R_2}P_{qq} \underset{x_1}{\otimes} {}^{R_1R_2}F_{q\bar{q}} + \sum_{R'} {}^{R_1R'}P_{qg} \underset{x_1}{\otimes} {}^{R'R_2}F_{g\bar{q}} \right](x_i, \boldsymbol{y}, \zeta_p, \mu_i)$$

From this one can obtain the evolution equation for $F^{11}_{q\bar{q}}$ as:

$$\frac{\partial}{\partial \log \mu_1^2} F^{11}_{q\bar{q}}(x_i, \boldsymbol{y}, \zeta_p, \mu_i) = a_s \left[\widetilde{P}_{qq} \underset{x_1}{\otimes} F^{88}_{q\bar{q}} + \frac{8}{3} \widetilde{P}_{qg} \underset{x_1}{\otimes} F^{\bar{3}3}_{g\bar{q}} - \frac{2}{9} {}^{8}\gamma_J^{(0)} \log \frac{\mu_1^2}{x_1^2 \zeta_p} F^{88}_{q\bar{q}} \right](x_i, \boldsymbol{y}, \zeta_p, \mu_i)$$

$\longrightarrow$ If the rhs. is negative this implies that evolution to higher scales drives $F^{11}_{q\bar{q}}$ negative!

Evaluating the rhs. of the DGLAP equation.

Using the same numerical setup as before we can check explicitly if evolution to higher scales drives $F^{11}_{q\bar{q}}$ negative:

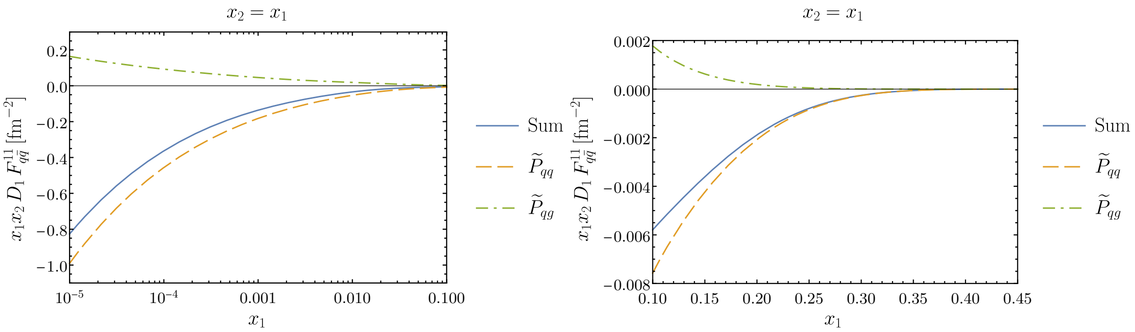

Evaluating the rhs. of the DGLAP equation.

Using the same numerical setup as before we can check explicitly if evolution to higher scales drives $F^{11}_{q\bar{q}}$ negative:

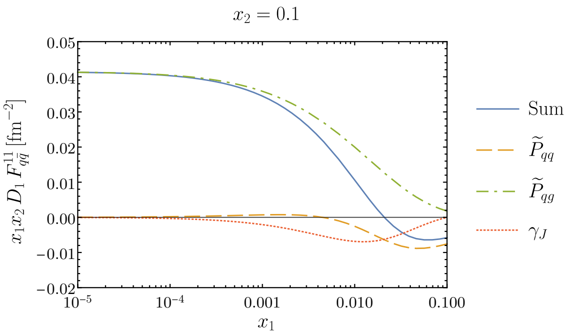

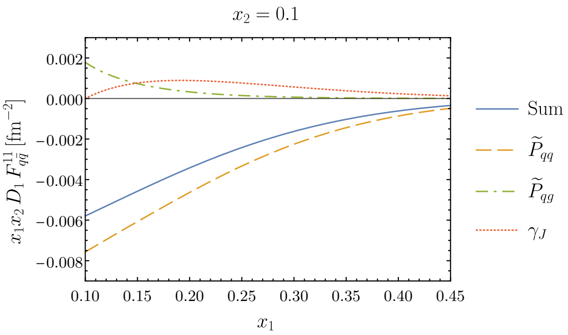

Evaluating the rhs. of the DGLAP equation.

Using the same numerical setup as before we can check explicitly if evolution to higher scales drives $F^{11}_{q\bar{q}}$ negative:

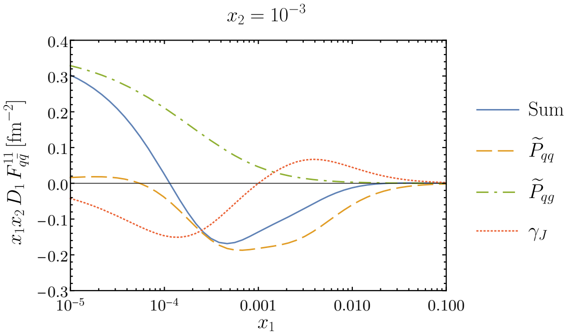

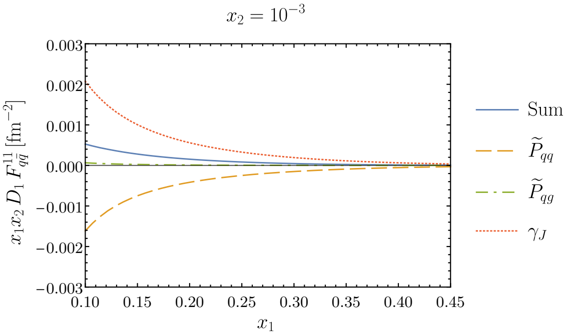

Summary.

Summary.

DPDs have a non-trivial colour structure with four open colour indices coupled to a colour singlet:

- Full colour structure can be decomposed in terms of distributions projected onto definite colour representations.
- Decomposition can be made in different "bases": t-, s-, and u-channel.

In the small-y limit DPDs can be calculated perturbatively, allowing us to study colour correlations:

- Already done at LO for all R_1R_2 and NLO for $R_1R_2 = 11$.
- Now also available at NLO for all R_1R_2.

For s-channel DPDs positivity bounds can be derived, whose validity can be checked explicitly using the perturbative small-y DPDs:

- NLO DPDs can violate positivity for certain kinematics.
- LO evolution to higher scales is not guaranteed to preserve positivity.

Summary.

DPDs have a non-trivial colour structure with four open colour indices coupled to a colour singlet:

- Full colour structure can be decomposed in terms of distributions projected onto definite colour representations.
- Decomposition can be made in different “bases”: t-, s-, and u-channel.

In the small-y limit DPDs can be calculated perturbatively, allowing us to study colour correlations:

- Already done at LO for all $R_1 R_2$ and NLO for $R_1 R_2 = 11$.
- Now also available at NLO for all $R_1 R_2$.

For s-channel DPDs positivity bounds can be derived, whose validity can be checked explicitly using the perturbative small-y DPDs:

- NLO DPDs can violate positivity for certain kinematics.
- LO evolution to higher scales is not guaranteed to preserve positivity.

Thank you for your attention!

Backup.

Rescaling of the rapidity parameter.

The rapidity parameters ζ_p and $\zeta_{\bar{p}}$ in this work are normalised as:

$$\zeta_p \zeta_{\bar{p}} = (2p^+ \bar{p}^-)^2 = s^2 \,,$$

which differs from the convention in the TMD case

$$\zeta \bar{\zeta} = x^2 \bar{x}^2 (2p^+ \bar{p}^-)^2 = Q^4 \,,$$

where the rapidity parameters are normalized w.r.t. the extracted parton, which would be awkward in the DPD case where parton momenta often appear in convolution integrals.

$\longrightarrow$ need to rescale the rapidity parameter in renormalisation factors and evolution kernels!

$\longrightarrow$ reason: can only depend on the plus-momentum $x_i p^+$ of the parton to which they refer!

From light-cone gauge diagrams to Wilson line diagrams in Feynman gauge.

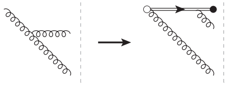

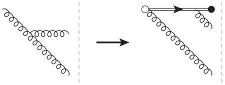

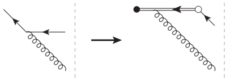

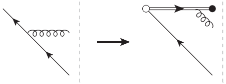

Kinematic limits of the small y DPDs.

Large $x_1 + x_2$: Plus distributions in the kernels lead to a $\log(1 - x_1 - x_2)$ enhancement in the DPDs.

- $g \to gg$, $g \to q\bar{q}$, and $q \to qg$

Small $x_1 + x_2$: For sufficiently steep PDFs the convolution integral in the small y DPD is dominated by z^{-2} terms in the kernels (in analogy to z^{-1} terms in DGLAP kernels).

- $g \to gg$, $g \to q\bar{q}$, and $q \to gg$ (in almost all colour channels)

Small x_1 or x_2: Corresponds to the small u and small $\bar{u}$ limit, with leading contributions going as u^{-1} and $\bar{u}^{-1}$ due to slow gluons.

- $g \to gg$, $q \to gg$, $g \to qg$ $(u^{-1}$ & $\bar{u}^{-1})$,
  $q \to qg$, and $q \to qq'$ $(\bar{u}^{-1})$

Find two sources for this behaviour in small y DPDs:

- Explicit u^{-1} and $\bar{u}^{-1}$ terms in the kernels.
- $(1 - z\bar{u})^{-1} \sim (k^+ - k_2^+)^{-1}$, $(1 - zu)^{-1} \sim (k^+ - k_1^+)^{-1}$ and similar terms.

Colour non-singlet evolution kernels.

The colour non-singlet evolution kernels have in the t-channel double DGLAP equation for ${}^{R_1 R_2}F_{q\bar{q}}$ on slide 18 have the following structure:

$$
{}^{RR'}P_{qa}(z,\zeta,\mu) = a_s \left[c_{RR'} \widetilde{P}_{qb}(z) + \delta_{RR'}\delta(1-z) \left(\frac{\gamma_q^{(0)}(\mu)}{2} + \frac{{}^{R}\gamma_J^{(0)}(\mu)}{2} \log \frac{\mu^2}{\zeta} \right) \right] + \mathcal{O}(a_s^2)
$$

where

$$
c_{11} = 1\,, \qquad c_{88} = -\frac{1}{8}\,, \qquad c_{8S} = \frac{\sqrt{5}}{4}\,, \qquad c_{8A} = \frac{3}{4}
$$

and

$$
\gamma_q(\mu) = 3\, C_F\, a_s(\mu) + \mathcal{O}(a_s^2)\,, \qquad {}^{1}\gamma_J(\mu) = 0\,, \qquad {}^{8}\gamma_J(\mu) = 2\, C_A\, a_s(\mu) + \mathcal{O}(a_s^2)
$$